

Giant increase in critical current density of $K_xFe_{2-y}Se_2$ single crystals

Hechang Lei and C. Petrovic

Condensed Matter Physics and Materials Science Department,
Brookhaven National Laboratory, Upton, NY 11973, USA

(Dated: November 5, 2018)

The critical current density J_c^{ab} of $K_xFe_{2-y}Se_2$ single crystals can be enhanced by more than one order of magnitude, up to $\sim 2.1 \times 10^4$ A/cm² by post annealing and quenching technique. A scaling analysis reveals the universal behavior of the normalized pinning force as a function of the reduced-field for all temperatures, indicating the presence of a single vortex pinning mechanism. The main pinning sources are three dimensional (3D) point-like normal cores. The dominant vortex interaction with pinning centers is via spatial variations in critical temperature T_c (" δT_c pinning").

PACS numbers: 74.25.Sv, 74.25.Wx, 74.25.Ha, 74.70.Xa

I. INTRODUCTION

Recently discovered iron-based superconductors¹ induce great interest in scientific community because of rather high T_c , proximity to the spin-density wave state and multiband nature of electronic transport.²⁻⁴ However, these materials also encourage potential technical applications due to high upper critical fields $\mu_0 H_{c2}$ and critical current densities J_c .⁴⁻⁷

In the family of iron-based superconductors, FeCh (Ch = S, Se, and Te, FeCh-11 type) materials have the simplest crystal structure, nearly isotropic high $\mu_0 H_{c2}$ and rather high J_c ,^{8,9} but their relatively low T_c impedes prospects for applications. Superconducting T_c was raised up to about 32 K in $A_xFe_{2-y}Se_2$ (A = K, Rb, Cs, and Tl, FeCh-122 type) iron selenide superconductors with rather high $\mu_0 H_{c2}$ (~ 56 T for $H \parallel c$ at 1.6 K).^{10,11} Preliminary results indicate that the J_c of $K_xFe_{2-y}Se_2$ is much lower when compared to iron arsenides or binary FeCh-11 type iron selenides.^{6,7,9,12-15} Post annealing and quenching treatment can induce metallic and superconducting state in as-grown and insulating $K_xFe_{2-y}Se_2$ crystals,¹⁶ yet current carrying characteristics of such materials are not known.

In this work, we report on the significant enhancement of critical current density in $K_xFe_{2-y}Se_2$ single crystals obtained via post-annealing and quenching process. We also give detailed insight into the vortex pinning mechanism. Main pinning sources are the 3D normal cores whereas dominant vortex interaction with pinning centers is via spatial variations in T_c .

II. EXPERIMENT

Details of crystal growth and structure characterization were reported elsewhere.¹² The as-grown crystals were sealed into Pyrex tube under vacuum ($\sim 10^{-1}$ Pa). The samples were annealed at 400 °C for 1h and quenched in the air as reported previously.¹⁶ Crystals were claved and cut into rectangular bars. Magnetization measurements were performed in a Quantum Design Magnetic Property Measurement System (MPMS-XL5).

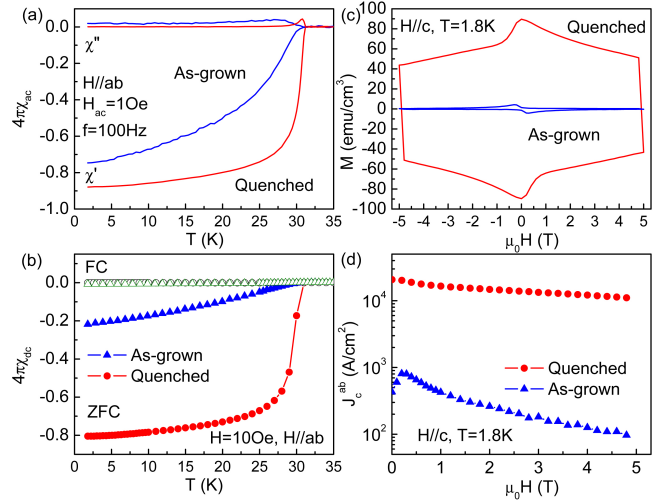


FIG. 1. Temperature dependence of the (a) ac and (b) dc magnetic susceptibility of as-grown and quenched $K_xFe_{2-y}Se_2$ crystals taken in $\mu_0 H = 0.1$ (ac) and 1 mT (dc) field, respectively. (c) Magnetization hysteresis loops of as-grown and quenched samples at 1.8 K for $H \parallel c$. (d) Superconducting critical current densities $J_c^{ab}(\mu_0 H)$ of as-grown and quenched samples.

III. RESULTS AND DISCUSSION

Calculated volume fractions from ac susceptibility at 1.8 K are rather similar, 75% for as grown and 88% for quenched crystal. However, the quenched crystal shows a very steep transition at 31 K and saturates at about 10 K whereas for as-grown sample the diamagnetic signal increases gradually with slightly lower T_c (Fig. 1(a)). The single sharp peak of $4\pi\chi''$ in quenched crystals (Fig. 1(a,b)) indicates more homogeneous superconducting state. The calculated volume fraction from dc susceptibility (Fig. 1(b)) significantly increased after quenching, consistent with previous results.¹⁶ Hence, post-annealing and quenching process significantly advances superconducting volume fraction in quenched $K_xFe_{2-y}Se_2$. The small volume fraction estimated from the FC curve suggests possible strong magnetic flux pinning effects.

Magnetic hysteresis loops (MHL) of quenched sam-

ple are much bigger and more symmetric (Fig. 1(c)). The pinning force is enhanced significantly and the bulk pinning is dominant when compared to the as-grown sample. The MHL of as-grown crystal is small and asymmetric, suggesting that the surface barrier may be important.^{17,18} Moreover, there is no fishtail effect up to 5 T which has been observed in S-doped $K_xFe_{2-y}Se_{2-x}S_x$ single crystal with $S = 0.99$ at low field and in FeAs-122 single crystals at high field.^{7,14,19–21}

The in-plane critical current density $J_c^{ab}(\mu_0H)$ for a rectangularly-shaped crystal with dimension $c < a < b$ when $H \parallel c$ is^{22,23}

$$J_c^{ab}(\mu_0H) = \frac{20\Delta M(\mu_0H)}{a(1 - a/3b)} \quad (1)$$

where a and b ($a < b$) are the in-plane sample size in cm, $\Delta M(\mu_0H)$ is the difference between the magnetization values for increasing and decreasing field at a particular applied field value (measured in emu/cm^3), and $J_c^{ab}(\mu_0H)$ is the critical current density in A/cm^2 . As shown in Fig. 1(d), the calculated $J_c^{ab}(0)$ for quenched sample from Fig. 1(c) is enhanced about 50 times when compared to as-grown sample. This can not be simply ascribed to the improvement of the superconducting volume fraction, because the volume fraction of quenched crystal is only about 4 times larger than the volume fraction of the as-grown crystal. Critical current values in quenched crystal are higher than that in $K_xFe_{2-y}Se_2$ crystals grown using the one-step technique and are the highest known J_c^{ab} among FeCh-122 type materials.¹⁵ The quenched sample also exhibits better performance at high field. The J_c^{ab} for quenched sample is still larger than $10^4 \text{ A}/\text{cm}^2$ at 4.8 T whereas for as-grown sample, it has decreased about one order of magnitude. The $J_c^{ab}(4.8T, 1.8K)$ is also larger than for $K_xFe_{2-y}Se_{2-z}S_z$ with $z = 0.99$.¹⁴

The temperature dependent symmetric curves for all MHLs imply that the bulk pinning dominates in the crystal at all temperatures. The hysteresis area decreases with the temperature suggesting gradual decrease of J_c^{ab} as the temperature is increased (Fig. 2(b)). The current carrying performance of quenched crystals is superior at all temperatures and fields when compared to crystals prepared using the one-step technique.¹⁵

In order to explain the mechanism of flux pinning in quenched sample, we studied the temperature and field dependencies of the vortex pinning force $F_p = \mu_0HJ_c$. Based on the Dew-Huges model,²⁴ if there is a dominant pinning mechanism then the normalized vortex pinning forces $f_p = F_p/F_p^{\max}$ from different measurement temperatures should overlap and a scaling law of the form $f_p \propto h^p(1-h)^q$ will be observed. Here h is the reduced field $h = H/H_{irr}$ and F_p^{\max} corresponds to the maximum pinning force. The irreversibility field μ_0H_{irr} is the magnetic field where $J_c^{ab}(T, \mu_0H)$ extrapolates to zero. The indices p and q provide the information about the pinning mechanism. As shown in Fig. 3(a), the normal-

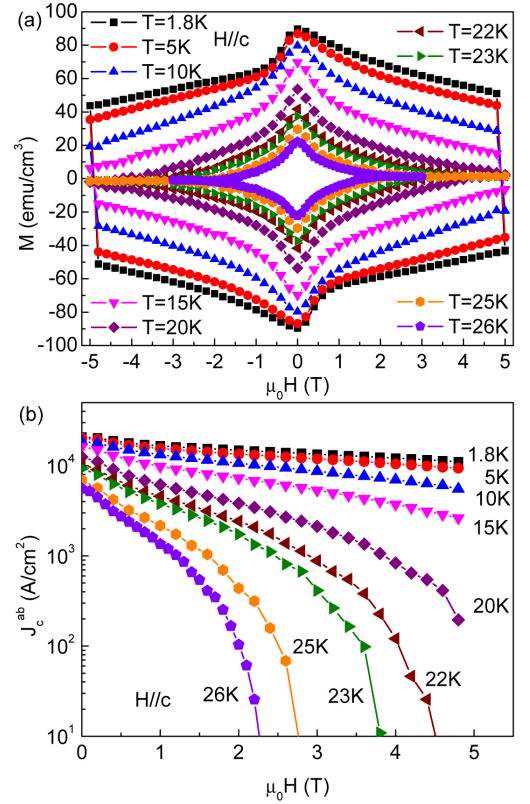


FIG. 2. (a) MHLs of quenched $K_xFe_{2-y}Se_2$ crystal for $H \parallel c$. (b) Magnetic field and temperature dependencies of superconducting critical current densities $J_c^{ab}(\mu_0H)$ for quenched $K_xFe_{2-y}Se_2$ crystal determined from MHLs.

ized curves of $f_p(h, T)$ for $T \geq 22 \text{ K}$ present a temperature independent scaling law. Using the scaling function $h^p(1-h)^q$, we estimate $p = 0.86(1)$ and $q = 1.83(2)$, respectively. The value of $h_{\max}^{fit} (= p/(p+q)) \approx 0.32$ is consistent with the peak positions ($h_{\max}^{\text{exp}} \approx 0.33$) of the experimental curves at different temperatures. Those values are close to expected values for core normal point-like pinning ($p = 1, q = 2$, and $h_{\max}^{fit} = 0.33$).²⁴ Moreover, for $T \leq 20 \text{ K}$, the H_{irr} can be estimated by F_p^{\max} location at $h_{\max} = 0.33$. Partial $f_p(h, T)$ curves measured between 10 and 20 K also exhibit the same scaling law, suggesting that core normal point-like pinning mechanism is dominant above 10 K. These point-like pinning center could come from the random distribution of Fe vacancies after quenching, similar to FeAs-122 type materials.^{7,19,20} On the other hand, the F_p^{\max} obeys the $F_p^{\max} \propto (\mu_0H_{irr})^\alpha$ scaling with $\alpha = 1.67(1)$ (inset of Fig. 3(a)), close to the theoretical value ($\alpha = 2$) for the core normal point-like pinning.²⁴ Moreover, as shown in Fig. 3(b), the temperature dependence of μ_0H_{irr} can be fitted by using $\mu_0H_{irr}(T) = \mu_0H_{irr}(0)(1-t)^\beta$ where $t = T/T_c$ and we obtained $\beta = 1.21(1)$, close to the characteristic value of 3D giant flux creep ($\beta = 1.5$).²⁵ Similar index has been observed in overdoped $Ba(Fe_{1-x}Co_x)_2As_2$.²⁶

Given the presence of 3D core pinning in quenched $K_xFe_{2-y}Se_2$ single crystals, it is important to distin-

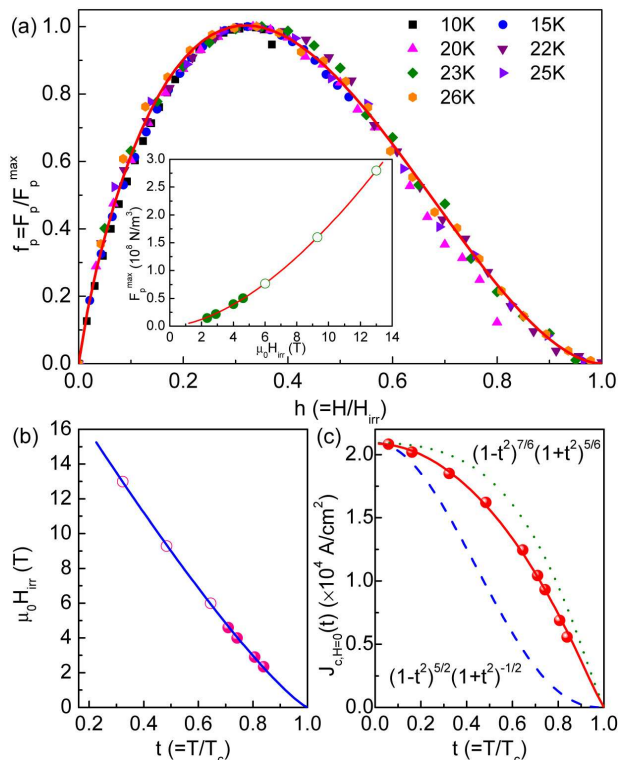


FIG. 3. (a) Reduced field dependence of normalized flux pinning force $f_p(h)$ at various temperatures. Solid line is the fitting curve using $f_p = Ah^p(1-h)^q$. Inset shows F_p^{\max} as a function of $\mu_0 H_{irr}$. The fitting result using $F_p^{\max} = A(\mu_0 H_{irr})^\alpha$ is shown as solid lines. (b) Reduced temperature dependence of $\mu_0 H_{irr}(t)$ with the solid line standing for the fitting result obtained by using the $(1-t)^\beta$ law. (c) Reduced temperature dependence of the $J_c(t)$ at zero field. The dotted, dashed and solid lines show the $J_{c,H=0}^{\delta T_c}(t)$, $J_{c,H=0}^{\delta l}(t)$ and the fitting result using $J_{c,H=0}(t) = xJ_{c,H=0}^{\delta T_c}(t) + (1-x)J_{c,H=0}^{\delta l}(t)$, respectively (see text). The measured and estimated $\mu_0 H_{irr}$ are shown as closed and open circles in inset of (a) and (b).

guish between the case of δT_c and δl pinnings. For type-II superconductors, vortices interact with pinning centers either via the spatial variations in the T_c (" δT_c pinning") or by scattering of charge carriers with reduced mean free path l near defects (" δl pinning").²⁷ These two pinning types have different temperature dependence and therefore result in different relationship be-

tween $J_c(t)$ and $t = T/T_c$ in the single vortex-pinning regime (low-field and zero-field regions). For δT_c pinning, $J_{c,H=0}^{\delta T_c}(t) = J_{c,H=0}(0)(1-t^2)^{7/6}(1+t^2)^{5/6}$ while for δl pinning, $J_{c,H=0}^{\delta l}(t) = J_{c,H=0}(0)(1-t^2)^{5/2}(1+t^2)^{-1/2}$.²⁸ As shown in Fig. 3(c), the $J_{c,H=0}(t)$ is between the two curves corresponding to δT_c and δl pinnings, respectively, but much closer and similar in shape to the δT_c -pinning curve. Using $J_{c,H=0}(t) = xJ_{c,H=0}^{\delta T_c}(t) + (1-x)J_{c,H=0}^{\delta l}(t)$, the experimental data can be fitted very well with $x = 0.74(2)$, suggesting that both δT_c and δl pinnings play roles in the quenched $K_x\text{Fe}_{2-y}\text{Se}_2$ single crystals, but the former mechanism is dominant. It also implies that the main pinning centers lead to the distribution of T_c in their vicinity or even might be non-superconducting like Y_2O_3 and Y-Cu-O precipitates in $\text{YBa}_2\text{Cu}_3\text{O}_{7-x}$ thin films.²⁹

Even though the J_c^{ab} of quenched $K_x\text{Fe}_{2-y}\text{Se}_2$ single crystals is still one or two order(s) smaller than that of other iron pnictide superconductors,^{7,19–21} post-annealing and quenching technique is an effective way to increase the J_c^{ab} of $K_x\text{Fe}_{2-y}\text{Se}_2$.

IV. CONCLUSION

In summary, we report giant increase in the J_c^{ab} of $K_x\text{Fe}_{2-y}\text{Se}_2$ single crystals by post-annealing and quenching technique. We demonstrate that quenched $K_x\text{Fe}_{2-y}\text{Se}_2$ crystals carry the highest observed J_c^{ab} among FeCh-122 type materials and exhibit good performance at high field. Detailed analysis of vortex pinning mechanism points out to the presence of a 3D point-like normal core pinning in quenched samples. Moreover, the analysis of temperature dependence of J_c^{ab} at zero field indicates that the δT_c pinning is dominant at measured temperature range.

V. ACKNOWLEDGEMENTS

Work at Brookhaven is supported by the U.S. DOE under Contract No. DE-AC02-98CH10886 and in part by the Center for Emergent Superconductivity, an Energy Frontier Research Center funded by the U.S. DOE, Office for Basic Energy Science.

¹ Y. Kamihara, T. Watanabe, M. Hirano, and H. Hosono, *J. Am. Chem. Soc.* **130**, 3296 (2008).
² Z.-A. Ren, G.-C. Che, X.-L. Dong, J. Yang, W. Lu, W. Yi, X.-L. Shen, Z.-C. Li, L.-L. Sun, F. Zhou, and Z.-X. Zhao, *EPL* **83**, 17002 (2008).
³ C. de la Cruz, Q. Huang, J. W. Lynn, J. Li, W. Ratcliff II, J. L. Zarestky, H. A. Mook, G. F. Chen, J. L. Luo, N. L. Wang, and P. Dai, *Nature* **453**, 899 (2008).

⁴ F. Hunte, J. Jaroszynski, A. Gurevich, D. C. Larbalestier, R. Jin, A. S. Sefat, M. A. McGuire, B. C. Sales, D. K. Christen, and D. Mandrus, *Nature* **453**, 903 (2008).
⁵ H. Q. Yuan, J. Singleton, F. F. Balakirev, S. A. Baily, G. F. Chen, J. L. Luo, and N. L. Wang, *Nature* **457**, 565 (2009).
⁶ J. Karpinski, N. D. Zhigadlo, S. Katrych, Z. Bukowski, P. Moll, S. Weyeneth, H. Keller, R. Puzniak, M. Tortello, D. Daghero, R. Gonnelli, I. Maggio-Aprile, Y. Fasano, Ø.

- Fischer, K. Rogacki, and B. Batlogg, *Physica C* **469**, 370 (2009).
- ⁷ H. Yang, H. Luo, Z. Wang, and H. H. Wen, *Appl. Phys. Lett.* **93**, 142506 (2008).
- ⁸ H. C. Lei, R. W. Hu, E. S. Choi, J. B. Warren, and C. Petrovic, *Phys. Rev. B* **81**, 094518 (2010).
- ⁹ C. S. Yadav and P.L. Paulose, *Solid State Commun.* **151**, 216 (2011).
- ¹⁰ J. Guo, S. Jin, G. Wang, S. Wang, K. Zhu, T. Zhou, M. He, and X. Chen, *Phys. Rev. B* **82**, 180520(R) (2010).
- ¹¹ E. D. Mun, M. M. Altarawneh, C. H. Mielke, V. S. Zapf, R. Hu, S. L. Bud'ko, and P. C. Canfield, *Phys. Rev. B* **83**, 100514(R) (2011).
- ¹² H. C. Lei and C. Petrovic, *Phys. Rev. B* **83**, 184504 (2011).
- ¹³ R. Hu, K. Cho, H. Kim, H. Hodovanets, W. E. Straszheim, M. A. Tanatar, R. Prozorov, S. L. Bud'ko, and P. C. Canfield, *Supercond. Sci. Technol.* **24**, 065006 (2011).
- ¹⁴ H. C. Lei and C. Petrovic, *Phys. Rev. B* **84**, 052507 (2011).
- ¹⁵ Z. S. Gao, Y. P. Qi, L. Wang, C. Yao, D. L. Wang, X. P. Zhang, and Y. W. Ma, arXiv:1103.2904 (2011).
- ¹⁶ F. Han, B. Shen, Z.-Y. Wang, and H.-H. Wen, arXiv:1103.1347 (2011).
- ¹⁷ M. Pissas, E. Moraitakis, D. Stamopoulos, G. Papavassiliou, V. Psycharis, and S. Koutandos, *J Supercond. Nov. Magn.* **14**, 615 (2001).
- ¹⁸ L. Zhang, Q. Qiao, X. B. Xu, Y. L. Jiao, L. Xiao, S. Y. Ding, and X. L. Wang, *Physica C* **445-448**, 236 (2006).
- ¹⁹ D. L. Sun, Y. Liu, and C. T. Lin, *Phys. Rev. B* **80**, 144515 (2009).
- ²⁰ A. Yamamoto, J. Jaroszynski, C. Tarantini, L. Balicas, J. Jiang, A. Gurevich, D. C. Larbalestier, R. Jin, A. S. Sefat, M. A. McGuire, B. C. Sales, D. K. Christen, and D. Mandrus, *Appl. Phys. Lett.* **94**, 062511 (2008).
- ²¹ R. Prozorov, N. Ni, M. A. Tanatar, V. G. Kogan, R. T. Gordon, C. Martin, E. C. Blomberg, P. Proumapan, J. Q. Yan, S. L. Bud'ko, and P. C. Canfield, *Phys. Rev. B* **78**, 224506 (2008).
- ²² C. P. Bean, *Phys. Rev. Lett.* **8**, 250 (1962).
- ²³ E. M. Gyorgy, R. B. van Dover, K. A. Jackson, L. F. Schneemeyer, and J. V. Waszczak, *Appl. Phys. Lett.* **55**, 283 (1989).
- ²⁴ D. Dew-Hughes, *Philos. Mag.* **30**, 293 (1974).
- ²⁵ Y. Yeshurun and A. P. Malozemoff, *Phys. Rev. Lett.* **60**, 2202 (1988).
- ²⁶ B. Shen, P. Cheng, Z. S. Wang, L. Fang, C. Ren, L. Shan, and H.-H. Wen, *Phys. Rev. B* **81**, 014503 (2010).
- ²⁷ G. Blatter, M. V. Feigel'man, V. B. Geshkenbein, A. I. Larkin, and V. M. Vinokur, *Rev. Mod. Phys.* **66**, 1125 (1994).
- ²⁸ R. Griessen, Hai-hu Wen, A. J. J. van Dalen, B. Dam, J. Rector, H. G. Schnack, S. Libbrecht, E. Osquiguil, and Y. Bruynseraede, *Phys. Rev. Lett.* **72**, 1910 (1994).
- ²⁹ A. O. Ijaduola, J. R. Thompson, R. Feenstra, D. K. Christen, A. A. Gapud, and X. Song, *Phys. Rev. B* **73**, 134502 (2006).